Skin-friction reduction with opposite-charged dielectric barrier discharge plasma actuators

Results in Engineering 26 (2025) 104611

Contents lists available at ScienceDirect

Results in Engineering

journal homepage: www.sciencedirect.com/journal/results-in-engineering

Research paper

Skin-friction reduction with opposite-charged dielectric barrier discharge plasma actuators

Atilla Altıntaş *, Lars Davidson, Shia-Hui Peng

Chalmers University of Technology, Division of Fluid Dynamics, Department of Mechanics and Maritime Sciences, Gothenburg, 412 96, Vastra Gotaland, Sweden

ARTICLE INFO

Keywords:
Drag reduction
DBD plasma actuators
Skin friction reduction
DNS
Plasma discharge

ABSTRACT

This study explores the potential of oppositely charged dielectric barrier discharge (DBD) plasma actuators to reduce skin friction in turbulent channel flow by generating wall-normal plasma jets. Leveraging the lightweight structure of electrodes, this technique presents a promising approach to minimizing aerodynamic drag on moving surfaces. A plasma force is applied to the bottom wall of the channel, targeting the suppression of organized flow structures inherent to turbulence. The investigation is conducted at a frictional Reynolds number $Re_\tau = 180$ using Direct Numerical Simulation (DNS), providing a detailed assessment of flow dynamics. The results demonstrate that wall-normal plasma jets, induced by spanwise-aligned actuators, achieve a modest reduction in skin friction drag, approximately 4%. This reduction highlights the viability of the method while underscoring the need for parameter optimization to enhance its effectiveness. The study provides insights into the mechanisms of drag reduction, emphasizing the influence of the plasma jet on turbulent structures. Future research is encouraged to refine actuator configurations and operating parameters to realize greater aerodynamic efficiency.

1. Introduction

Plasma jet flow is a technique used to reduce the skin friction drag on the surface of a body moving through a fluid. The technique involves the use of plasma discharge to generate a jet of fluid in actuator-aligned direction that interacts with the flow field and modifies it in a way that reduces the skin friction drag [1].

Recent studies have demonstrated the effectiveness of wall-aligned plasma jet flow in reducing drag in different flow scenarios, including turbulent boundary layers [2]. The ability to generate body forces without moving parts makes them attractive for aerodynamic flow control in various applications, including boundary-layer manipulation and turbulent flow control.

Early studies on plasma-based flow control demonstrated the feasibility of streamwise-aligned plasma jets for reducing skin friction and delaying flow separation [3]. Later, oscillatory plasma jets explored, which showed promise in modifying turbulence structures to suppress near-wall streaks and quasi-streamwise vortices [4]. Studies such as those by Shyy et al. [5] provided an analytical model to describe the plasma-induced force distribution. This model has since been validated against experiments [1] and developed more accurate plasma actuator implementations.

In the context of skin-friction reduction, several approaches using plasma actuators have been proposed [6–8] demonstrated the potential of plasma-generated streamwise vortices in turbulent boundary layers, showing moderate drag reduction. A comprehensive review also provided by [9]. These studies primarily focused on parallel plasma jet actuation, where the induced force aligns with the main flow direction. However, the potential of wall-normal plasma jet flow, created using plasma actuators, in terms of its drag reduction capabilities remains an area that requires investigation [6,10].

The presented study deviates from the usual parallel plasma jet by creating a wall-normal plasma jet [1,6], marking an important change. This approach distinguishes our research, offering a novel perspective on the use of plasma actuators for drag reduction. By exploring this unconventional method, our aim is to shed light on its potential benefits in aerodynamic control and boundary layer manipulation, contributing valuable insights to the field and possible applications mainly in aviation.

The effectiveness of this technique depends on several factors, such as the size and shape of the plasma actuator, the applied voltage, the frequency of the discharge, and the properties of the fluid. The plasma actuator generates a plasma discharge that creates a jet of fluid that

* Corresponding author.
E-mail address: altintas@itu.edu.tr (A. Altıntaş).

https://doi.org/10.1016/j.rineng.2025.104611
Received 27 November 2024; Received in revised form 27 February 2025; Accepted 9 March 2025

Available online 14 March 2025

interacts with the flow field and modifies it in a way that reduces the skin friction drag.

Previous studies have identified the dominant structures at low Reynolds numbers in the near-wall region as streamwise velocity streaks and quasi-streamwise vortices [1,11]. In this study, we investigated the effectiveness of a wall-normal applied plasma jet in a turbulent channel flow at a low Reynolds number by applying a force to the bottom wall of the channel. We believe that the method outlined here could serve as a reference point for studies at higher Reynolds numbers.

Our goal was to suppress the formation or interaction of organized flow structures in the flow. This study was performed for a frictional Reynolds number of $Re_\tau = 180$. We examined the skin friction drag reduction capabilities of the wall-normal plasma jet by analyzing the applied force and no-force cases. To verify the results, we investigated changes in streak formations using tools such as velocity fluctuations and two-point correlations. Our findings suggest that wall-normal plasma jet flow has the potential to reduce skin friction drag in turbulent flow. The plasma actuator was found to suppress the formation and interaction of streamwise vortices, leading to a reduction in the drag.

The present study investigates an alternative method for skin-friction reduction by utilizing oppositely charged dielectric barrier discharge (DBD) plasma actuators to generate wall-normal plasma jets. Unlike conventional plasma actuators that primarily induce streamwise-aligned body forces, this approach directly modifies near-wall turbulence structures by influencing the development of quasi-streamwise vortices and velocity streaks.

Previous research has largely focused on plasma actuation strategies that generate parallel plasma jets or oscillatory forcing to alter turbulence dynamics. Studies on streamwise-aligned plasma jets have demonstrated their ability to reduce skin friction by modifying the turbulent boundary layer. However, the effects of wall-normal plasma forcing through opposing DBD plasma actuators remain largely unexplored. The novelty of this study lies in investigating how this specific plasma actuator configuration affects turbulence dynamics and drag reduction.

The paper is structured as follows: it begins with an overview of the numerical method, followed by the derivation and validation of the plasma force generated by a single DBD actuator. The subsequent section demonstrates the configuration of the opposing actuators and introduces the created wall-jet flow. Finally, the paper presents and discusses the results, followed by concluding remarks.

2. Direct numerical simulations

A flow solver with an implicit, two-step time-advancement finite volume method is used [13]. Central differencing is used in space and the Crank-Nicolson scheme is used in the time domain. When the Navier-Stokes the equation is discretized for u_i it can be written as,

$$u_i^{n+1} = u_i^n + \Delta t H\left(u_i^n, u_i^{n+1}\right) - \frac{1}{\rho}\alpha\Delta t\frac{\partial p^{n+1}}{\partial x_i} - \frac{1}{\rho}(1-\alpha)\Delta t\frac{\partial p^n}{\partial x_i} \tag{1}$$

where $H\left(u_i^n, u_i^{n+1}\right)$ includes convection, the viscous and the source terms, and $\alpha = 0.5$ (Crank-Nicolson). Equation (1) is solved which gives u_i^{n+1} that does not satisfy continuity. An intermediate velocity field is computed by subtracting the implicit part of the pressure gradient, i.e.

$$u_i^* = u_i^{n+1} + \frac{1}{\rho}\alpha\Delta t\frac{\partial p^{n+1}}{\partial x_i}. \tag{2}$$

Taking the divergence of Eq. (2) requiring that continuity (for the face velocities which are obtained by linear interpolation) should be satisfied on level $n+1$, i.e. $\partial u_{i,f}^{n+1}/\partial x_i = 0$, we obtain

$$\frac{\partial^2 p^{n+1}}{\partial x_i \partial x_i} = \frac{\rho}{\Delta t\alpha}\frac{\partial u_{i,f}^*}{\partial x_i}. \tag{3}$$

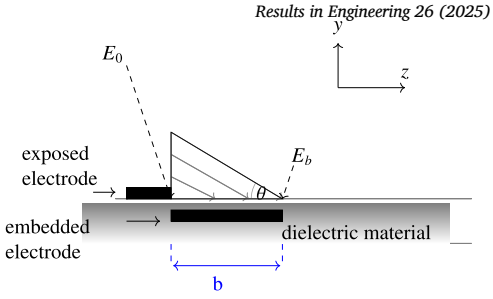

Fig. 1. Shyy model illustration. Electric field strength, $E(y,z)$.

The numerical procedure at each time step can be summarized as follows.

1. Solve the discretized filtered Navier-Stokes equation for u, v and w.
2. Create an intermediate velocity field u_i^* from Eq. (2).
3. The Poisson equation (Eq. (3)) is solved with an efficient multigrid method [14].
4. Compute the face velocities (which satisfy continuity) from the pressure and the intermediate velocity as

$$u_{i,f}^{n+1} = u_{i,f}^* - \frac{1}{\rho}\alpha\Delta t\left(\frac{\partial p^{n+1}}{\partial x_i}\right)_f. \tag{4}$$

5. Step (i) to (iv) is performed till convergence (normally two or three iterations) is reached. The convergence for the velocities is 10^{-7} and 10^{-5} for pressure. The residuals are computed using the $L1$ norm and they are scaled with the integrated streamwise volume flux (the continuity equation) and momentum flux (momentum equations).
6. Next time step.

Note that although no explicit dissipation is added to prevent odd-even decoupling, an implicit dissipation is present. The intermediate velocity field is computed at the *cell centers* (see Eq. (2)) subtracting a pressure gradient. Then, after having solved the pressure Poisson equation, the face velocity field is computed, and the pressure gradient at the *faces* (see Eq. (4)) is added. This is very similar to the Rhie-Chow dissipation [15].

3. Methodology

3.1. Shyy model for single DBD actuator

The Shyy model creates an electric field vector, **E**, generated by a DBD plasma actuator, which is given as:

$$E(y,z) = E_0 - \frac{E_0 - E_b}{b}z^+ - \frac{E_0 - E_b}{b\tan(\theta)}y^+ \tag{5}$$

Equation (5) is divided into wall-normal and spanwise components, multiplied by a factor Dc

$$E_z(y,z) = Dc\,E(y,z)\cos\theta, \tag{6}$$

$$E_y(y,z) = Dc\,E(y,z)\sin\theta. \tag{7}$$

The parameter Dc is defined as the ratio of the electrical force to the inertial force, given by the equation $Dc = \frac{q_0 E_0 \delta}{\rho u_\tau^2}$. Here, q_0 represents the maximum electron charge density. E_0 corresponds to the maximum electric field strength, which decreases along the embedded electrode until it reaches the breakdown strength E_b at the other edge (refer to Fig. 1). The quantities δ, ρ, and u_τ represent half the channel height, fluid density, and friction velocity, respectively.

In this study, the values chosen are $E_0 = 1.0$ and $E_b = 0.1$. The length of the plasma area is denoted by b, and the height of the plasma area is set as $b\tan(\theta)$. In the study conducted by Shyy et al. [5], the plasma

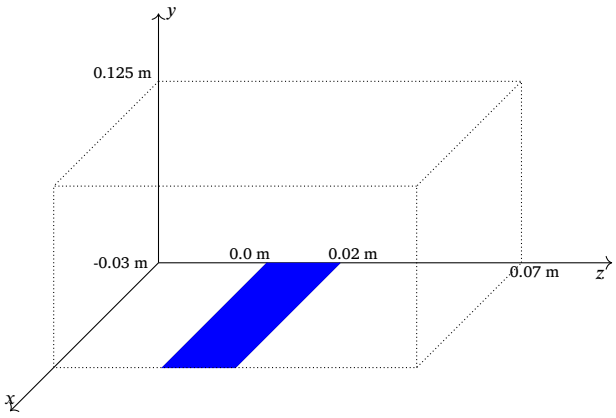

Fig. 2. The location of the embedded electrode for the single DBD actuator.

area was created in both the wall-normal (y) and streamwise (x) directions. However, in this study, the actuators are oriented in the spanwise direction, resulting in the force being generated in the y and z directions.

3.2. Validation of the Shyy model

The numerical model is compared to experimental data in a stationary flow with a single DBD actuator. Both experimental and computational fluid dynamics (CFD) results were obtained using a single DBD actuator. The experimental study, conducted by Benard et al. [4], applied a voltage of 12 kV and an AC frequency of 1000 Hz.

A two-dimensional study in a channel is performed, as shown in Fig. 2. Equations (6) and (7) are solved in two dimensions (along the y and z directions), and the solution is iterated until a steady state is reached. Slip boundary conditions are applied in the actuator-aligned direction (z) and at the top boundary (high y). The fluid viscosity, $\nu = 1.81 \times 10^{-5}; m^2/s$, and density, $\rho = 1.25; kg/m^3$, are specified. Only the spanwise-directed component of the force is considered ($\theta = 0$), so only Equation (6) is applied, and $E_y = 0$ (i.e., Equation (2) is set to zero). This approach is similar to the model proposed by Greenblatt et al. [3], where a mean body force acts only in the plasma-aligned direction. The computational domain has dimensions of 125 mm × 100 mm, as shown in Fig. 1, with grid sizes of 98×298 ($y \times z$) for the wall-normal and plasma-aligned directions, respectively. The minimum and maximum grid sizes are $\Delta y_{min} = 0.00025$ m and $\Delta y_{max} = 0.0025$ m, with a stretching factor of $y = 1.35$ in the wall-normal direction. The grid size in the plasma-aligned direction is $\Delta z = 0.00033$ m. The oscillating force is applied in the plasma region ($0.0 < z < 0.02$ m, $0.0 < y < 0.0028$ m). The length of the plasma is $b = 20$ mm, and its location is illustrated in blue in Fig. 2. The plasma region is discretized using 30×6 cells in the plasma-aligned and wall-normal directions, respectively.

The predicted velocities of the ionized airflow exhibit a very similar behavior compared to the experimental data, as shown in Figs. 3 and 4. The presence of the plasma region creates a negative wall-normal velocity upstream of the actuator and a positive wall-normal velocity downstream of the actuator (Figs. 3(a) and 4(a)). The negative area entrains the flow towards the wall, while the positive area downstream of the actuator creates a wall jet that propagates downstream with a velocity parallel to the actuator (Figs. 3(b) and 4(b)). Large vorticity is generated in the shear layer above the actuator (Figs. 3(c) and 4(c)). In the experimental study, the maximum plasma-aligned velocity is 1.8 m/s, and the wall-normal velocity is half that, at 0.9 m/s. The magnitude of vorticity is 1400. In the numerical study, we obtain similar velocity and vorticity fields compared to the experiments.

3.3. Wall-normal jet actuator design by opposing DBD actuators

The actuator that is used in this study is consist of two identical single DBD plasma actuators positioned opposite to each other with a gap area in between Fig. 5. The purpose of this arrangement is to generate a wall-normal jet flow in the middle of the actuator, when a high-voltage AC signal is applied to the actuators Figs. 6(a)-6(d).

4. Multiple actuator configuration for DNS

4.1. DNS settings

A DNS is performed to investigate the effects of multiple plasma actuators aligned in the spanwise direction. The aim is to generate a controlled body force to manipulate the flow.

A constant volumetric driving force is used in the streamwise momentum equation by which the frictional Reynolds number, $Re_\tau = 180$ is prescribed [14]. Periodic boundary conditions are used in the streamwise and spanwise directions, while the usual no-slip boundary conditions are enforced at the walls. The domain size is $2\pi\delta \times 2\delta \times \pi\delta$ with grid size $98 \times 98 \times 194$ in the streamwise, wall-normal and spanwise directions, respectively. The grid resolution is $\Delta x^+ \approx 11.5, \Delta z^+ \approx 2.9$, and a stretching factor of 1.03 is applied in the wall-normal direction, resulting in $y^+_{min} = 0.8$ and $y^+_{max} = 7.5$. The non-dimensional time step is kept below $\Delta t^+ = \Delta t u_\tau^2/\nu = 0.6$. The solver progressed through 10,000 time steps for no-force cases, with each step requiring approximately 8.177×10^{-4} simulation time units.

We would like to note that the grid resolution used in this study is sufficient for DNS at $Re_\tau = 180$, as demonstrated by a comparison with our previous study [1], where a finer spanwise resolution was employed. The results for both the mean velocity profile and velocity fluctuations obtained with the present coarser grid are in close agreement with those from the finer grid. Furthermore, both meshes yield results that are consistent with well-established DNS data in the literature [17]. These observations confirm that the present mesh resolution is adequate for capturing the key turbulence characteristics and drag reduction effects without significant loss of accuracy.

4.2. Multiple actuator design

The specific configuration of the actuators is shown in Fig. 7. To simplify the analysis, only the spanwise component of the body force is considered, which means the force acts solely in the spanwise direction ($\theta = 0$ or $F_y = 0$). This simplification allows for a focused examination of the influence of the plasma actuators on the flow behavior.

The length of the plasma area, denoted as b, is chosen to be 5 computational cells. This corresponds to a dimensionless length of $b^+ = \frac{bu_\tau}{\nu} = 14.5$ for a given friction Reynolds number of $Re_\tau = 180$. This defines the maximum width of the plasma region in the spanwise direction for a single DBD actuator.

To space the plasma actuators appropriately, a spanwise spacing, S_p, is implemented in between opposed plasma areas, which is set equal to twice the length of the single plasma area (b^+). There are also a spacing between the 9 actuator pairs, which is equal to %20 of a single plasma area (b^+). The spacing, resulting in a total of 9 plasma actuators being employed in this study Fig. 7(a). The specific arrangement and distribution of the actuators are determined based on this configuration. The creation of the force in the flow field is given in the Fig. 7(b).

For the simulations, a dimensionless parameter Dc is set to a value of 1.0, representing the ratio of the electrical force to the inertial force in the system. This choice of Dc influences the intensity of the generated body force and its impact on the flow.

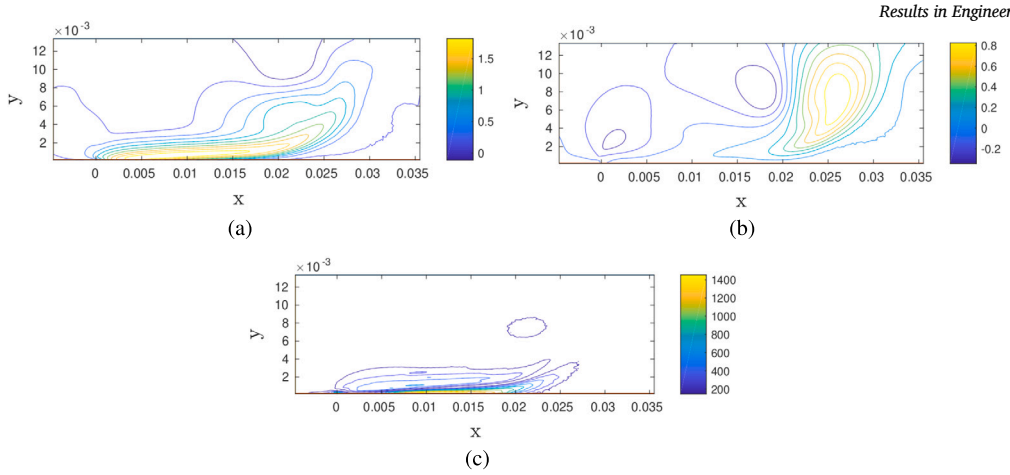

Fig. 3. Experiments. [4] (a) Plasma-aligned velocity, w. (b) wall-normal velocity, v. (c) vorticity.

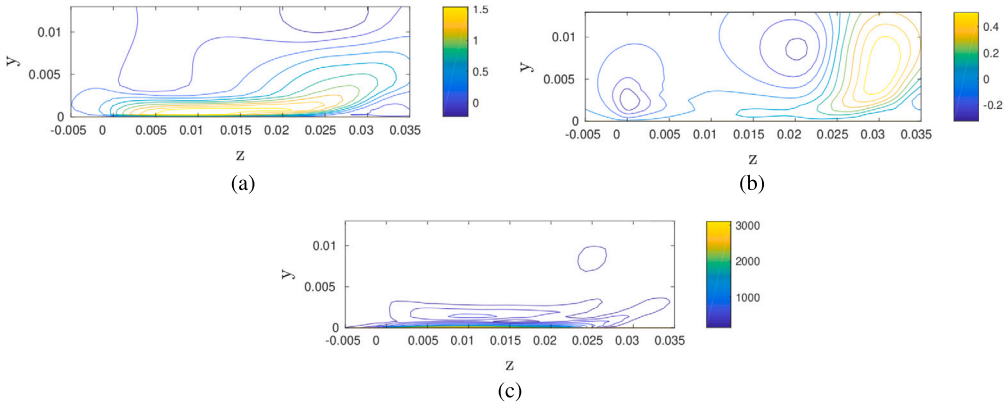

Fig. 4. Numerical study. (a) Plasma-aligned velocity, w. (b) wall-normal velocity, v. (c) vorticity.

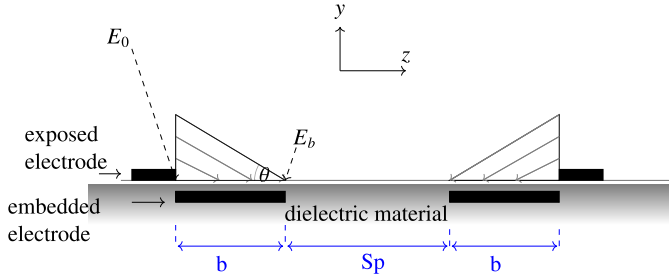

Fig. 5. Illustration of opposed actuators to create a wall-normal jet.

5. Results, discussion and limitations

5.1. Results

The analysis reveals that the implementation of the plasma actuators results in a modest reduction in drag, approximately 4%. Although the drag reduction achieved in this study is relatively low, it provides valuable insights into the potential effects and limitations of the employed plasma actuator configuration.

Fig. 8(a) presents the mean velocity for the force and the no-force cases, compared with DNS data [17]. We have not observed any change on the mean flow. A slightly lower streamwise velocity fluctuations, u_{rms}, and wall-normal velocity fluctuations, v_{rms}, are observed for the applied force case compared to the no-force case (Fig. 8(b) and 8(c)). For the applied force case, the spanwise velocity fluctuations, w_{rms}, are lower for the force applied case compared to no-force case Fig. 8(d)).

Fig. 9, presents the Reynolds shear stresses for the force and no-force cases. A reduction approximately at $y^+ = 20$ till $y^+ = 90$ is observed, which results a reduction on drag.

The presence of a minimum in the profiles of the wall-normal two-point velocity correlation in the spanwise direction, $R_{vv}(z)$, is indicative of the existence of streamwise vortical structures in the wall region [16,18]. These structures can be characterized by a mean vortex structure, which is defined based on the time-averaged positions of the local minimum and maximum of the streamwise root mean square (rms) vorticity. The occurrence of the minimum in $R_{vv}(z)$ is directly related to the average spanwise distance across a vortex.

In Fig. 10(a), where the values of $R_{vv}(z)$ are plotted for the south wall, it is observed that there is a decrease in the correlation for $y^+ = 10$, while preserving the same y^+ location, when compared to the no-force cases. This implies that the applied force influences the strength of the mean streamwise vortices near the wall, while the mean separation between vortices remains largely unaffected. In other words, the force alters the intensity of the vortical structures without significantly affecting their spatial arrangement.

Fig. 10(b) illustrates the values of $R_{vv}(z)$ for the upper half of the channel. The values for the applied force cases closely align with the values obtained in the no-force cases.

5.2. Discussion

The present study examines the impact of wall-normal plasma jets, generated by oppositely charged dielectric barrier discharge (DBD)

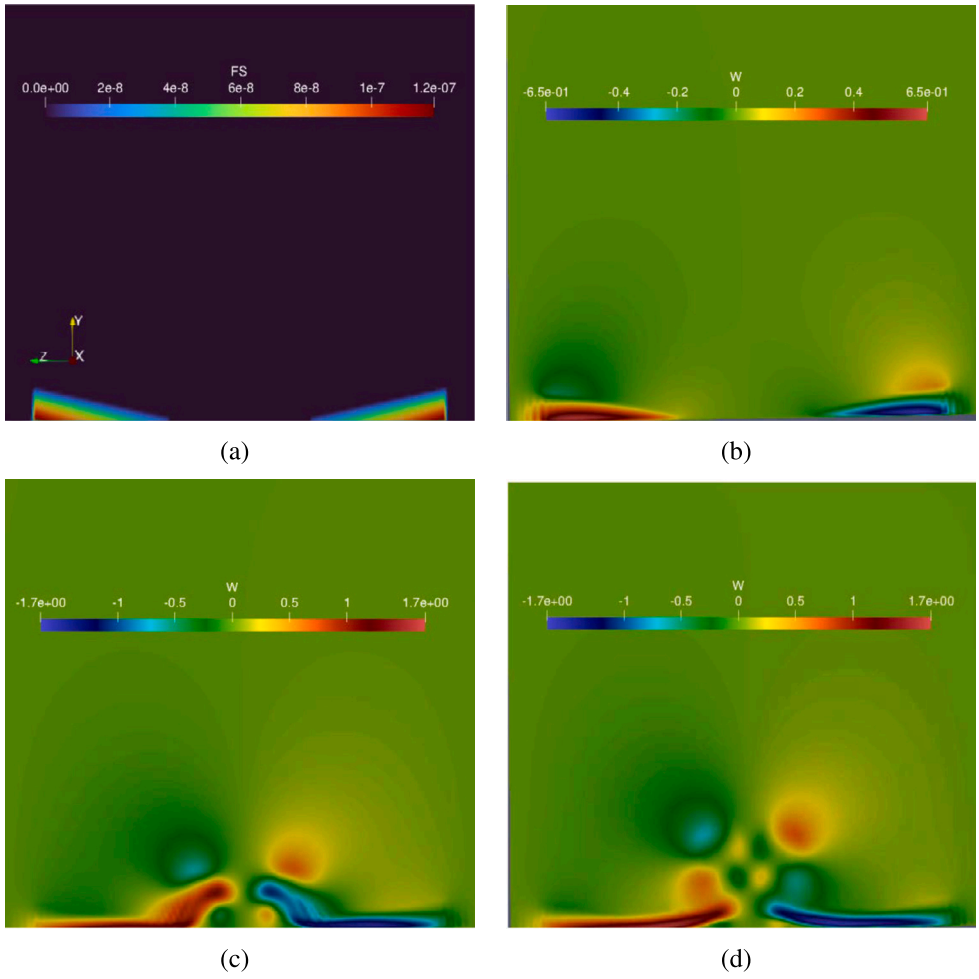

Fig. 6. Created force and flow. (a) Force. (b)-(d) Plasma-aligned velocity evolution with time, which shows the creation of the wall-jet.

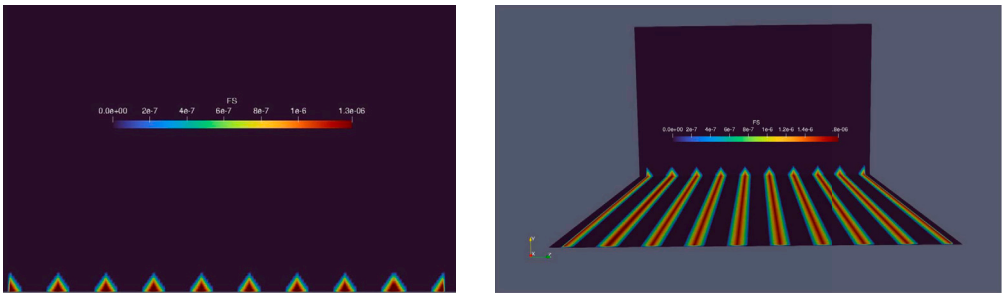

Fig. 7. The plasma force is created in the south wall of the channel by using multiple actuators. (a) 9 actuator pairs are used. (b) Applied force.

plasma actuators, on skin-friction reduction in turbulent channel flow. The results indicate that applying the plasma force leads to a modest reduction in drag, approximately 4%. The findings highlight the influence of plasma-induced body forces on modifying turbulence characteristics, which is consistent with previous studies on plasma-based flow control mechanisms [1,4].

The analysis of two-point velocity correlations reveals that the applied plasma force alters the intensity of streamwise vortical structures near the wall without significantly affecting their spatial distribution. This suggests that the wall-normal plasma jet primarily influences turbulence by modifying near-wall streak interactions rather than inducing large-scale structural changes in the boundary layer [12]. The decrease in turbulent fluctuations and Reynolds shear stress supports the conclusion that plasma actuation suppresses the regeneration of turbulence structures, thereby reducing skin friction.

Although the achieved drag reduction is lower than that reported for spanwise oscillating plasma actuators [1], the approach presented here offers an alternative mechanism for influencing turbulence. The advantage of wall-normal plasma jets lies in their ability to directly target turbulence structures in the wall region, which differs from traditional streamwise and spanwise plasma jet configurations. The ability to generate local flow modifications without requiring large-scale actuator placement or excessive power input suggests that this technique could be further optimized for practical aerodynamic applications.

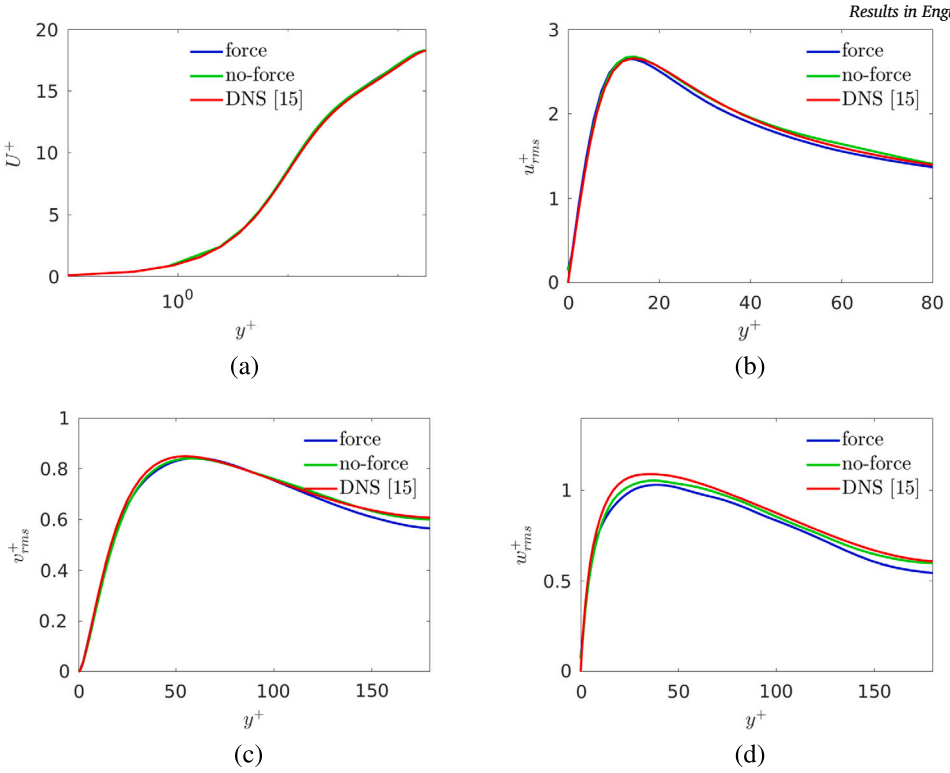

Fig. 8. Mean and fluctuation velocities. (a) Mean velocity. (b) Streamwise velocity rms, u^+_{rms}. (c) Wall-normal velocity rms, v^+_{rms}. (d) Spanwise velocity rms, w^+_{rms}.

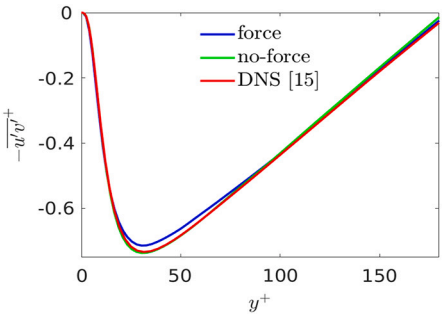

Fig. 9. Reynolds shear stress.

5.3. Limitations of DBD plasma actuators in practical applications

While dielectric barrier discharge (DBD) plasma actuators have demonstrated potential for flow control and drag reduction, several practical limitations must be considered when evaluating their real-world aerodynamic applications.

One of the most critical limitations of DBD plasma actuators is the voltage required for effective operation. Plasma actuators typically function at voltages in the range of kilovolts (kV), which raises power consumption, safety, and integration into existing aerodynamic designs [19].

The performance of DBD plasma actuators is highly dependent on environmental factors such as humidity, temperature, and atmospheric pressure. These conditions influence the ionization process and can lead to inconsistent plasma discharge characteristics, affecting the actuator's efficiency and reliability in real-world applications [9].

Scaling up DBD plasma actuators to cover larger aerodynamic surfaces presents a significant challenge. While single-surface actuators have demonstrated localized flow control effects, ensuring efficiency and uniform performance across larger surfaces is more complex [1].

6. Conclusion

This study investigates the effectiveness of oppositely charged dielectric barrier discharge (DBD) plasma actuators in reducing skin-friction drag through the generation of wall-normal plasma jets. Direct Numerical Simulations (DNS) were conducted for a turbulent channel flow at $Re_\tau = 180$ to analyze the impact of plasma-induced forcing on turbulence modification and drag reduction. The results indicate that this novel plasma actuation method leads to a measurable reduction in wall shear stress, primarily by altering near-wall turbulence structures.

The findings demonstrate that the applied plasma force influences turbulence by suppressing Reynolds shear stress and modifying the intensity of streamwise vortices in the near-wall region. Unlike traditional streamwise or spanwise plasma actuation methods, which rely on direct momentum injection parallel to the flow direction, the wall-normal plasma jets introduced in this study affect turbulence regeneration mechanisms by reducing streak interactions. The analysis of velocity fluctuations and two-point correlation functions confirms that the plasma-induced forcing alters the near-wall cycle responsible for turbulence production.

Although the achieved drag reduction is modest, approximately 4%, the results suggest that wall-normal plasma forcing provides an alternative mechanism for influencing near-wall turbulence. The effectiveness of this approach could be further improved by optimizing actuator configurations, placement, and forcing parameters. Additionally, the observed turbulence modification trends indicate potential for hybrid actuation strategies that combine wall-normal and spanwise forcing for enhanced drag reduction.

The influence of fractional-order derivatives in modeling heat transport phenomena, which may have potential applications in plasma-induced flow control [20]. Future research could extend the present study to higher Reynolds numbers and investigate the long-term stability of plasma-induced turbulence suppression. Experimental validation at larger scales, along with the integration of adaptive plasma control strategies, could further improve the feasibility of this method for real-world aerodynamic applications. The insights gained from this study

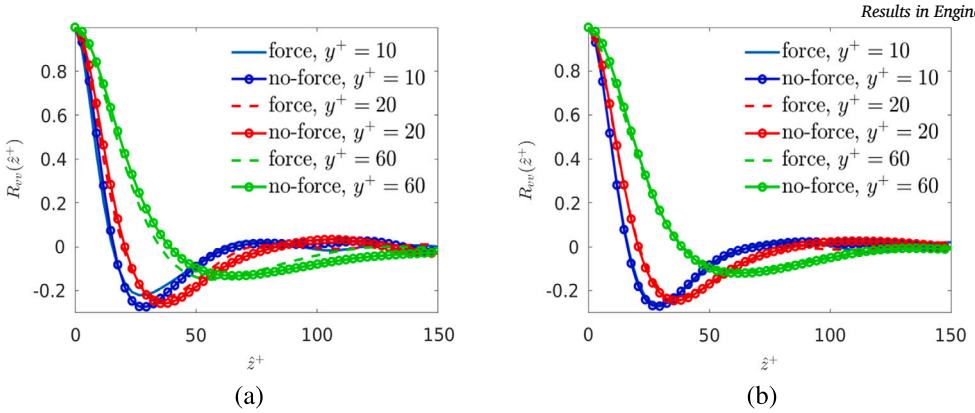

Fig. 10. Wall-normal two-point velocity correlation for force applied case. (a) South wall. (b) North wall.

contribute to the broader understanding of plasma-based flow control and highlight the potential of alternative plasma forcing techniques in turbulence management.

CRediT authorship contribution statement

Atilla Altıntaş: Writing – review & editing, Writing – original draft, Visualization, Validation, Software, Methodology, Investigation, Formal analysis, Data curation, Conceptualization. **Lars Davidson:** Writing – review & editing, Supervision, Methodology, Conceptualization. **Shia-Hui Peng:** Writing – review & editing, Supervision.

Declaration of competing interest

The authors declare that they have no known competing financial interests or personal relationships that could have appeared to influence the work reported in this paper.

Data availability

Data will be made available on request.

References

[1] A. Altıntaş, L. Davidson, S.-H. Peng, Direct numerical simulation of drag reduction by spanwise oscillating dielectric barrier discharge plasma force, Phys. Fluids 32 (7) (2020).
[2] S. Yadala, M.T. Hehner, J. Serpieri, N. Benard, M. Kotsonis, Plasma-based forcing strategies for control of crossflow instabilities, AIAA J. 59 (9) (2021) 3406–3416, https://doi.org/10.2514/1.J060101.
[3] D. Greenblatt, T. Schneider, C.Y. Schüle, Mechanism of flow separation control using plasma actuation, Phys. Fluids 24 (7) (2012).
[4] N. Benard, M. Caron, E. Moreau, Evaluation of the Time-Resolved EHD Force Produced by a Plasma Actuator by Particle Image Velocimetry-a Parametric Study, Journal of Physics: Conference Series, vol. 646, IOP Publishing, 2015, p. 012055.
[5] W. Shyy, B. Jayaraman, A. Andersson, Modeling of glow discharge-induced fluid dynamics, J. Appl. Phys. 92 (11) (2002) 6434–6443.
[6] X. Cheng, C. Wong, F. Hussain, W. Schröder, Y. Zhou, Flat plate drag reduction using plasma-generated streamwise vortices, J. Fluid Mech. 918 (2021) A24.
[7] K. Karthikeyan, R. Harish, Enhanced aerodynamic performance of naca4412 airfoil through integrated plasma actuator and Gurney flap flow control, Results Eng. 25 (2025) 103977.
[8] T.-L. Phan, T.T. Nguyen, T.H.T. Nguyen, Optimization of unsteady jet control flow method for aerodynamic drag reduction of heavy truck model, Results Eng. 22 (2024) 102167.
[9] M. Abdullah, M.T. Galib, M.S.A. Khan, T. Rahman, M.M. Hossain, Recent advancements in flow control using plasma actuators and plasma vortex generators, Heat Transf. 53 (8) (2024) 4244–4267.
[10] S. Pasch, T. Fridlender, M.T. Hehner, N. Benard, J. Kriegseis, Combined and simultaneous electro-optical diagnostics for oscillatory plasma discharges, in: AIAA AVIATION 2023 Forum, 2023, p. 4027.
[11] A. Altıntaş, L. Davidson, S.-H. Peng, A new approximation to modulation-effect analysis based on empirical mode decomposition, Phys. Fluids 31 (2) (2019) 025117.
[12] L. Agostini, M. Leschziner, On the departure of near-wall turbulence from the quasi-steady state, J. Fluid Mech. 871 (2019) R1.
[13] L. Davidson, S.-H. Peng, Hybrid LES-RANS: a one-equation SGS model combined with a $k-w$ model for predicting recirculating flows, Int. J. Numer. Methods Fluids 43 (9) (2003) 1003–1018.
[14] P. Emvin, L. Davidson, Development and implementation of a fast large eddy simulations method, Tech. Rep., Dept. of Thermo and Fluid Dynamics, Chalmers University of Technology, Gothenburg, 1997.
[15] C.M. Rhie, W.L. Chow, Numerical study of the turbulent flow past an airfoil with trailing edge separation, AIAA J. 2 (1983) 1525–1532.
[16] A. Altıntaş, L. Davidson, Direct numerical simulation analysis of spanwise oscillating Lorentz force in turbulent channel flow at low Reynolds number, Acta Mech. 228 (2017) 1269–1286.
[17] J. Jiménez, J.C. Del Alamo, O. Flores, The large-scale dynamics of near-wall turbulence, J. Fluid Mech. 505 (2004) 179–199.
[18] J. Kim, P. Moin, R. Moser, Turbulence statistics in fully developed channel flow at low Reynolds number, J. Fluid Mech. 177 (1987) 133–166.
[19] P. Sujar-Garrido, M. Becerra, R. Örlü, Efficiency assessment of a single surface dielectric barrier discharge plasma actuator with an optimized Suzen–Huang model, Phys. Fluids 34 (4) (2022).
[20] A. Rasheed, M.S. Anwar, Numerical computations of fractional nonlinear Hartmann flow with revised heat flux model, Comput. Math. Appl. 76 (10) (2018) 2421–2433.